RESEARCH ARTICLE

The effects of long-term freezing–thawing on the strength properties and the chemical stability of compound solidified/stabilized lead-contaminated soil

Zhongping Yang[1,2,3] · Keshan Zhang[1,2,3] · Xuyong Li[1,2,3] · Shupei Ren[1,2,3] · Peng Li[1,2,3]

Abstract

Solidification/stabilization (S/S) is the prevalent remediation technology for the treatment of heavy metal contaminated soils (HMCS). However, under the stress of complex surrounding environments, S/S effectiveness tends to deteriorate and freezing–thawing is one of the most influential natural forcings. The different proportions of cement, lime, and fly ash were used as the compound curing agents to treat solidified/stabilized HMCS with varying levels of lead contamination. The resulting samples were subjected to up to 180 freeze–thaw cycles (F-T) (1 day per cycle). Unconfined compressive strength (UCS) tests and semi-dynamic leaching tests were performed after F-T to explore the strength evolution of compound solidified/stabilized lead-contaminated soils (Pb-CSCS) and the chemical stability of the lead within. The results show that the F-T duration changes the strength deterioration mechanism of Pb-CSCS under F-T. There has been a shift in the main influencing factor from the promoted curing agent hydration by short-term F-T to the structural damage of the specimen induced by prolonged F-T. The variations in leachate pH, lead leachability, and diffusion ability with progressing F-T revealed a degradation effect of the changes in the physical states of water and crack propagation brought by F-T. These unfavorable changes in soil structure and chemistry reduce the acid resistance of Pb-CSCS. Notably, fly ash and cement facilitate the strength maintenance of Pb-CSCS under long-term F-T conditions. Curing formulations that included both cement and fly ash significantly increased the UCS of treated soils by up to 80.5% (3 F-T) under short-term F-T. In contrast, the curing formulation without fly ash lost 51.8% of its strength after 180 F-T conditions. For lead stabilization, cement and especially lime are favored. The results showed a 25% increase in the total proportion of lime and cement in the curing agent formulation, leading to a 41.4% reduction of lead leaching risk.

Keywords Solidification/stabilization · Long-term freeze–thaw cycle · Compound curing agent · Strength evolution · Lead leachability · Deterioration mechanism

✉ Xuyong Li
  lixuyong@cqu.edu.cn

1 School of Civil Engineering, Chongqing University, Chongqing 400045, China

2 Key Laboratory of New Technology for Construction of Cities in Mountain Area (Chongqing University), Ministry of Education, Chongqing 400045, China

3 National Joint Engineering Research Centre for Prevention and Control of Environmental Geological Hazards in the TGR Area Chongqing University, Chongqing 400045, China

Introduction

Soil heavy metal contamination is a widespread environmental problem caused by recent global industrialization (Ashraf et al. 2019; Bai et al. 2021a; Tang et al. 2019). Lead contamination is currently one of the most severe and widespread problems of inorganic soil pollution, which has led to over 902,000 deaths and 21.7 million years of healthy life lost worldwide (Brady and Weil 2016; Hou et al. 2020a; Kumar et al. 2020). About one-third of the world's children are affected by lead poisoning, and about 800 million children have lead levels of 5 ug/dl or above in their blood, including 31.23 million in China (IHME 2020).Consequently, the effects of heavy metal contaminated soil (HMCS) to persons and the environment should be given careful consideration,

and comprehensive remediation is urgently required (Bai et al. 2021b; Zhang et al. 2019).

Solidification/stabilization (S/S) is now a widespread remediation procedure for heavy metal-contaminated sites. Aside from S/S, physical (Gu et al. 2022; Liu et al. 2022) and biological (Liu et al. 2021a; Sharma et al. 2020) remediation methods involving stripping-removal and degradation of contaminants in soil are the more desirable nature-based eco-friendly solutions (Pervaiz et al. 2023; Zheng et al. 2022). Nevertheless, these methods generally suffer from insufficient economics and slow remediation processes (Cao et al. 2023; Wang et al. 2022). In developing countries such as China, the urgent land need for rapid urbanization requires economical and effective contaminated site remediation, which has hampered their promotion (CAEPI 2020; Li 2019b). Correspondingly, S/S is a mature technology with a good remediation effect and high efficiency. It also improves the mechanical properties of the remediated site soil, which is favorable for landfill and construction projects (Chen et al. 2017; Hou and Al-Tabbaa 2014; Hou et al. 2016; Liu et al. 2021b; Wang et al. 2018, 2016).

When using S/S, however, the heavy metals in the soil are immobilized rather than fundamentally removed (Gong et al. 2018). It has raised concerns about the long-term efficacy of S/S remediation in complex surrounding environments. Available studies have certified that the stability of the S/S is closely affected by the surrounding environment (Shen et al. 2019; Wang et al. 2019; Wiles 1987), such as freeze–thaw cycles (F-T) (Aldaood et al. 2014; Eskişar et al. 2015; Hotineanu et al. 2015; Wang et al. 2015; Wei et al. 2015a, b), high saline groundwater (Liu 2014; Liu et al. 2015), acid rain (Du et al. 2012, 2014), and alternating wet-dry action (Li et al. 2014; Zha et al. 2013). Among them, soil freezing and thawing is a widespread climate phenomenon on a global scale and has significant impacts on soil properties. The average multi-year seasonal permafrost area in the northern hemisphere covers 50.5% of its total land area and even reaches 81% in extremely cold years (Gao 2021). It is especially true for China, where 53.5% of the country's territory is seasonally frozen (Yang et al. 2020a).

Studies have shown that F-T not only affects the physical properties of the soil but also alters its biochemical properties (Hotineanu et al. 2015; Shahidi et al. 2019). Consequently, it will inevitably affect S/S stability and could even cause remediation to fail completely. In cases discussing the effects of F-T on soil mechanical properties, the unconfined compressive strength (UCS) of solidified/stabilized clayey sand was reduced by more than 60% (Shahidi et al. 2019). A loss of 55% to 70% was found in the tangent modulus of the cement-treated soil after one F-T (Ding et al. 2018). Meanwhile, soil porosity increases as F-T duration increases, as does the leaching concentration of heavy metals in stabilized/solidified contaminated soil (He et al. 2021).

In most of the available studies (Hou et al. 2020b), however, only short-term F-T tests have been applied to the S/S soils, which is insufficient to investigate their long-term performances in terms of mechanical strength and heavy metal immobilization. Actually, the long-term durability of solidified/stabilized HMCS is sensitive to changes in environmental conditions (Ouhadi et al. 2021). Studies have confirmed that the UCS of Pb-CSCS was reduced by more than 38% under 90 F-T compared with 7 F-T and soil permeability was also nearly fourfold higher (Yang et al. 2019). After 90 F-T, the soil lost more than half of its cohesion, and the solute longitudinal migration coefficient of saturated soil was 23 times greater than that of soil without F-T (Yang et al. 2021).

However, most of these studies have focused on the effects of F-T on the strength characteristics of the solidified/stabilized HMCS and the stability of heavy metals, while little attention has been paid to the mechanisms of F-T on the curing agent components. Meanwhile, the few studies that focus on curing agents only used a single curing agent to stabilized/solidified HMCS, such as cement, lime, and fly ash (Deng 2017). Meeting the requirement of simultaneous superiority of various mechanical and chemical performances is difficult (Dermatas and Meng 2003; Li et al. 2021; Liu et al. 2019). Several studies have confirmed that (Wang et al. 2011) composite remediation by incorporating different kinds of curing agents improved both the mechanical and environmental performances due to the complementary remediation characteristics of these curing agents (Pu et al. 2020; Yi et al. 2012).

Therefore, this study utilized cement, lime, and fly ash mixed in different proportions as the composite curing agents for lead-contaminated soil composite remediation. The compound solidified/stabilized lead-contaminated soils (Pb-CSCS) were subjected to up to 180 F-T (1 day per cycle) before UCS and semi-dynamic leaching tests. Using F-T duration, curing agent formulation, and levels of lead contamination as variables, the main goals of this study are to investigate (1) the long-term mechanical performance, (2) the risks of lead leaching, and (3) the mechanisms behind how the performance evolutions of Pb-CSCS in a long-term F-T environment.

Methodology

Materials and specimen preparation

Materials

The contaminated soils were artificially prepared to ensure the consistency and reproducibility of their mechanical properties and pollution characteristics. The clay used in this study was obtained from a building site located in Jiangjin

District, Chongqing, southwestern China. It was a reddish-brown soil collected from the top 0.5 to 1.5 m of strata, and being used after drying, impurity removal, and screening. Its basic physical properties and chemical compositions are shown in Tables 1 and 2.

Based on the previous works, three curing agent formulations were selected to facilitate the simultaneous maintenance of superior multiple engineering properties under F-T (Deng 2017; Li 2019a; Yang et al. 2020a, b). The compound curing agents were composed of cement, lime, and fly ash at the ratios of 2.5%, 5%, and 5% (C2.5S5F5), 5%, 2.5%, and 2.5% (C5S2.5F2.5), and 5%, 5%, and 0% (C5S5) of dry soil weight, respectively. Chemical components of the curing agents obtained by XRF are shown in Table 2.

The contaminant of interest is lead. To improve solubility and avoid the interference of extraneous ions in the remediation process, lead was added to the soil in the form of $Pb(NO_3)_2$ mixed with deionized water. Three lead content (0.5%, 1%, 1.5%) and seven F-T levels (0, 3, 7, 14, 30, 90, 180 cycles) were set, according to previous study (Yang et al. 2019). The sample preparation scheme is presented in Table 3.

Specimen preparation

Uncontaminated soils and the compound curing agents were dried in an oven at 100 °C for 24 h before the grinding and screening process. Specimen moisture was controlled to 120% of the soil's optimum water content. The lead nitrate solution was remolded with deionized water to achieve both the required contamination levels and specimen moisture. The contaminated soil was then prepared with the target lead concentration by stirring weighed dry soil and lead nitrate solution homogeneously with a magnetic stirrer. After the contaminated soil samples were kept sealed in a thermostat with constant humidity for 30 days, the compound curing agents were added for its remediation. The resulting mixture was molded into columns 39.1 mm in diameter and 80 mm in length at 95% of the maximum soil density, then tightly wrapped with plastic film and placed in a standard curing box for 28 days. Specimen preparation processes were completed promptly to prevent water loss from the contaminated soil. The experimental process flowsheet of this study is shown in the Fig. 1.

Table 1 Basic physical properties of uncontaminated soil

Physical properties	Liquid limit (%)	Plastic limit (%)	Plasticity index (I_P)	Optimum water content (%)	Maximum dry density (g/cm^3)
Soil	29.7	17.2	12.1	19.52	1.93

Table 2 Chemical composition of uncontaminated soil and curing agents

Composition (wt%)	CaO	SiO$_2$	Al$_2$O$_3$	MgO	Fe$_2$O$_3$	SO$_3$	Na$_2$O	K$_2$O	TiO$_2$	Others
Soil	1.46	58.83	23.65	1.02	12.43	-	-	0.77	1.09	0.75
Cement	58.01	22.26	8.87	3.66	3.79	1.04	0.20	1.34	0.51	0.33
Lime	84.23	3.1	3.1	4.32	0.29	–	–	–	–	4.96
Fly ash	1.73	39.65	21.42	3.68	9.17	–	–	–	–	24.35

Table 3 Summary of the experimental scheme

F-T Test	Groups	F-T duration (cycles)	Curing agent formulation	Lead content
Short-term F-T	1	0	C5S2.5F2.5, C2.5S5F5, C5S5	0.5%, 1.0%, 1.5%
	2	3		
	3	7		
	4	14		
Long-term F-T	5	30		
	6	90		
	7	180		

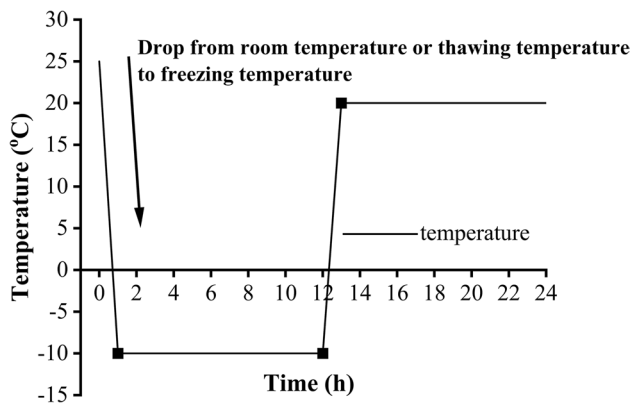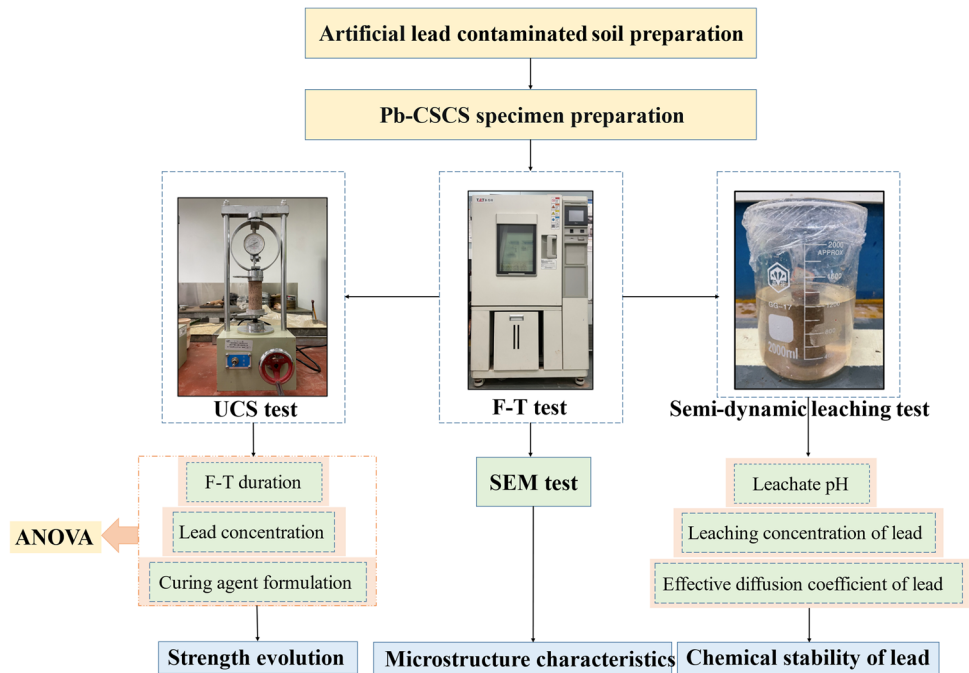**Fig. 1** Experimental process flowsheet

Fig. 2 Temperature control curve of single F-T

Test programs

F-T test

F-T tests were performed using a high-low temperature alternating test chamber (TC401, Chongqing Taisite Test Instrument Co. Ltd.). As shown in Fig. 2, each F-T refers to cooling the treated specimens from room temperature to −10 °C and freezing them for 11 h, then heating them to 20 °C and thawing them for 11 h. After completing the F-T tests, the specimens were transferred from the test box and air-dried for subsequent use.

UCS test

UCS tests were used to determine the effect of F-T, curing agent formulation, and lead concentration on the strength behavior of Pb-CSCS. The tests were performed according to the Geotechnical Testing Technology using a YYW-2 strain-controlled unconfined pressure apparatus (Shen and Zhang 2013). The load was applied by turning the hand-wheel, and the axial strain was generated at a rate of 1 to 3%/min. Loading continued until the strain continued to develop by 3 to 5% after the load values reached their peak, or until 20% strain when no peak load values occurred (Gao et al. 2014). The compression process of a single specimen was controlled within 8 to 10 min.

Semi-dynamic leaching

Semi-dynamic leaching tests were performed on all Pb-CSCS at 1% lead concentration and subjected to 0, 30, or 90 F-T cycles according to ASTM C1308-08 (ASTM 2008). The systematic flow diagram of the test processing is shown in Fig. 3.

An acetic acid solution (pH = 2.88) applied in with a ratio of 10: 1 (mL/cm^2) to the specimen surface area was used as the leaching solution. After measuring the initial pH of the leaching solution, the specimens were placed on the porous stones at the bottom of the beakers, and then the lips of the beakers were wrapped with plastic wrap. The specimens were transferred to beakers containing fresh leaching solutions after the 2-h initial soak. The leachate obtained from the immersion was acidified with concentrated nitric

Fig. 3 The systematic flow diagram of semi-dynamic leaching
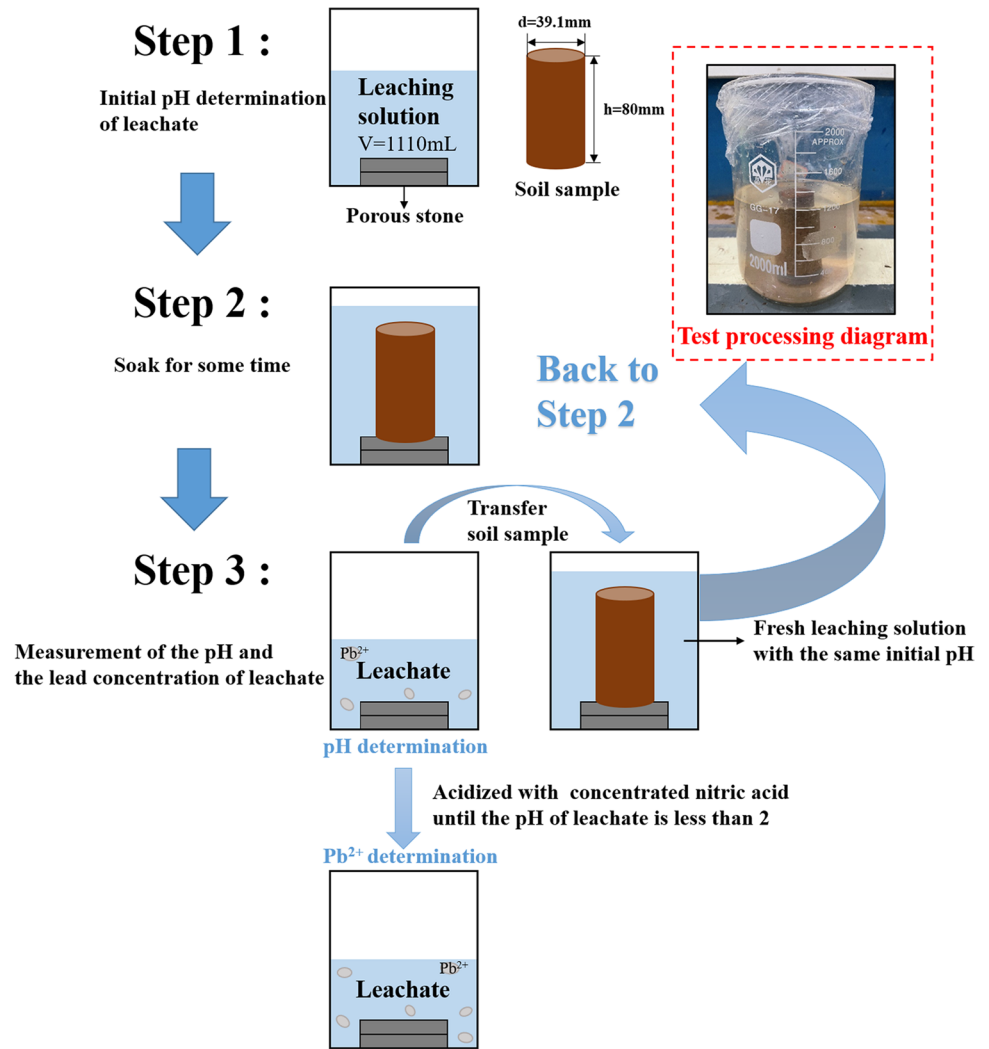
acid until its pH was less than 2 for the lead concentration measurement. Repeated operations were performed in the 5th h and 17th h, respectively. Afterward, the operations of leachate renewal and lead concentration measurement were repeated at 24-h intervals. The entire semi-dynamic leaching process for each sample lasted 11 days (Liu et al. 2013). Each set of tests was conducted in duplicate and the average lead concentrations were reported. Table 4 shows the semi-dynamic leaching test scheme.

Equation (1) (Liu et al. 2013) was used to calculate the cumulative dissolved mass of lead: where A_{max} is the cumulative dissolved mass of lead (mg), C_i is the lead concentration of the ith leachate (mg/L), and V_i is the volume of leachate (L).

$$A_{max} = \sum C_i \times V_i, (i = 1, 2, 3, \dots, 13) \tag{1}$$

The effective diffusion coefficient of lead in Pb-CSCS (D_e) was determined by Eq. (2):

$$D_e = \prod \left[\frac{\frac{a_n}{A_0}}{(\Delta t)_n} \right]^2 \left[\frac{V}{S} \right]^2 T, (n = 1, 2, 3, \dots, 13) \tag{2}$$

where D_e is the effective diffusion coefficient (cm²/s), a_n is the dissolved contaminants in leaching interval n (mg), A_0 is the initial content of pollutants in the samples (mg), V is the volume of the samples (cm³), S is the surface area of samples (cm²). $(\Delta t)_n$, $T = [(t_n^{1/2} + t_{n-1}^{1/2})/2]$, and t_n are the

Table 4 Time interval of leachate renewal in semi-dynamic leaching tests

Leaching interval (n)	1	2	3	4	5	6	7	8	9	10	11	12	13
nth leaching time (h)	2	5	17	24	24	24	24	24	24	24	24	24	24
Cumulative time (h)	2	7	24	48	72	96	120	144	168	192	216	240	264

time interval, the average time, and the cumulative leaching time of the nth leaching, respectively (ANSI 2019).

Three-way analysis of variance

Analysis of variance (ANOVA) is an important element of mathematical statistics for testing the significance of differences between the means of two or more samples. Multifactor ANOVA uses the decomposability of the mathematical model to decompose the conditional error (between groups) and random error (within groups) from the total variance, and compare them to find out the main factors affecting the test results.

In this paper, a three-way ANOVA model with no interaction effects and repeated tests was used to analyze the main factor affecting the UCS. As shown in Table 5, F-T duration, curing agent formulation, and lead content are denoted as factors A, B, and C, respectively. Each factor corresponds to different factor levels. A total of 36 tests were conducted under the level combination of $(A_i B_j C_k)$, and the test results were labeled as y_{ijk}, where i, j, and k represent the levels of factors A, B, and C, respectively.

The command for three-way ANOVA without interaction is shown as Eq. (3):

$$[p, t] = anovan(x, group) \tag{3}$$

where x is the value of all tests at the level combination of $(A_i B_j C_k)$, and p returns the three probability values corresponding to each of the three factors. $p < 0.01$ indicates a significant effect of the corresponding factor on the test results, otherwise, it is excluded from the main influencing factors (Guo 2015).

The sum of squares between groups is used to measure the effect of a factor on a test indicator. The relationship strength (R^2) of the investigated factors on the test indicator is reflected by the magnitude of the between-group sum of squares as a proportion of the total sum of squares, defined as Eq. (4) (Zhong et al. 2015):

$$R^2 = \frac{S_L^2}{S_T^2} \tag{4}$$

where S_L^2 denotes the sum of squares for factor L, and S_L^2 denotes the total sum of squares.

The effect size ($\hat{\alpha}_i$) reflects the magnitude of the pure effect of the ith level of factor L on the test indicators, as shown in Eq. (5) (Zhong et al. 2015):

$$\hat{\alpha}_i = \bar{y}_i - \bar{y} \tag{5}$$

where $\bar{y}_i$ represents the mean of the test indicators at the ith level of factor L, and $\bar{y}$ represents the mean of all test indicators. A higher effect size indicates a greater impact of the level on the test indicator.

SEM test

The morphology of Pb-CSCS was observed with scanning electron microscopy (SEM) using a Zeiss Gemini 300. For better observation and accurate images, the diced samples (5 mm × 5 mm × 5 mm) for the SEM test were taken from the freshly exposed surface of Pb-CSCS that were subjected to F-T. After drying at a temperature of 50 °C for 48 h, the samples were sprayed with gold for 30 s to enhance their conductivity.

Results and discussion

UCS of Pb-CSCS under long-term F-T

The effect of F-T duration

The UCS of the Pb-CSCS as a function of F-T times is shown in Fig. 4. Intuitively, the UCS of Pb-CSCS after long-term F-T all shared a similar pattern of variation, as the UCS generally decreased with increasing F-T times. As the temperature alters between positive and negative under F-T, the volume difference caused by changes in the three states of water in the soil structure increases the squeezing

Table 5 Three-way ANOVA data structure table for the UCS of Pb-CSCS under F-T

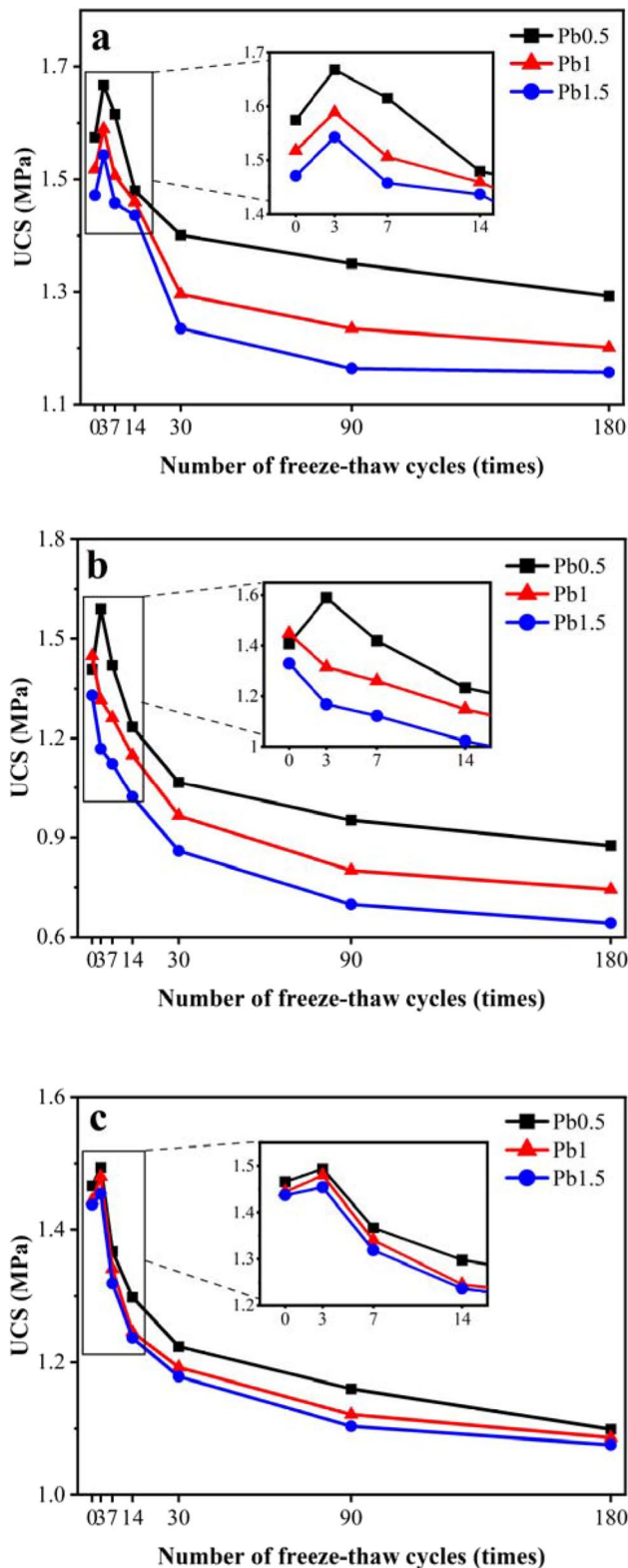| F-T duration	Factor	Factor level			
		1	2	3	4
Short-term	A(F-T duration)	0	3	7	14
	B(Curing agent formulation)	C2.5S5F5	C5S2.5F2.5	C5S5	-
	C(Lead content)	0.5%	1%	1.5%	-
Long-term	A(F-T duration)	0	30	90	180
	B(Curing agent formulation)	C2.5S5F5	C5S2.5F2.5	C5S5	-
	C(Lead content)	0.5%	1%	1.5%	-

Fig. 4 UCS of Pb-CSCS subjected to different F-T times: **a** C5S2.5F2.5, **b** C5S5, and **c** C2.5S5F5

effect on the surrounding soil particles (Fig. 5). This leads to displacement and destruction of the particles and, consequently, changes in the morphology of the soil pores. At the microscopic level, the minerals in the clay are negatively charged and surrounded by polar water molecules. Negative temperature causes the internally bound water to freeze, disrupting the original electrochemical equilibrium. Meanwhile, the unfrozen water is continually attracted to the surrounding soils, creating a new equilibrium (Deng 2017). This could also be responsible for the continuous expansion and contraction deformation within the soil, which eventually causes the strength deterioration shown when under long-term F-T.

As shown in Fig. 4a and c, the UCS of the specimens shows enhancement at a low number of F-T (0 to 3). This could be attributed to the fact that, given the generally strong hydrophilicity of alkaline curing agents, some water would absorb on the surface of alkaline curing agents to form a water film during the curing stage of the specimens instead of fully reacting with the curing agents (Cao et al. 2013). As F-T progressing, the changes in physical state of water promoted further hydration reactions of curing agents. Main reactions of cement, lime, and fly ash are shown in Tables 6, 7, and 8, respectively (Peng 2006; Yu and Xu 2018). The hydration products C-S–H ($3CaO \cdot 2SiO_2 \cdot 3H_2O$), C_3AH_6 ($3CaO \cdot Al_2O_3 \cdot 6H_2O$), $Ca(OH)_2$, and $CaCO_3$ fill the pores on the surface of the soil particle and eventually wrap the particles to form a blocky cohesive body (Yang 2003; Yu et al. 1989). At the same time, the large amount of active metal oxides (CaO, MgO, etc.) contained in cement and lime reacts with the soil particles through ion exchange, hardening, and carbonation. Moreover, active silica and alumina in fly ash combined with CaO to produce hydraulic binders, which significantly improved the curing ability of cement and lime. Short-term F-T reduced the gaps and the thicknesses of the bonded water film between soil particles in this manner, resulting in a tighter soil structure and increased soil strength (Yousuf et al. 1995).

The effect of curing agent formulation

The UCS of Pb-CSCS with the varying curing agent formulation is depicted in Fig. 6. All the UCS were found to meet the US recommendation of 0.35 MPa (USEPA 1996). Increasing cement content contributed to a significant enhancement in the UCS under F-T. For example, the UCS of C5S2.5F2.5 was 12.3% higher than that of C2.5S5F5 at a lead content of 1% when subjected to 7 F-T (Fig. 6b). In addition, the presence of fly ash effectively improved the strength and stability of the specimen under F-T. Compared to C5S5 (7 F-T, 1% lead), the UCS of C2.5S5F5 and C5S2.5F2.5 increased by 6.3% and 19.4%, respectively. It has to do with the fact that only 1.73% of calcium oxide

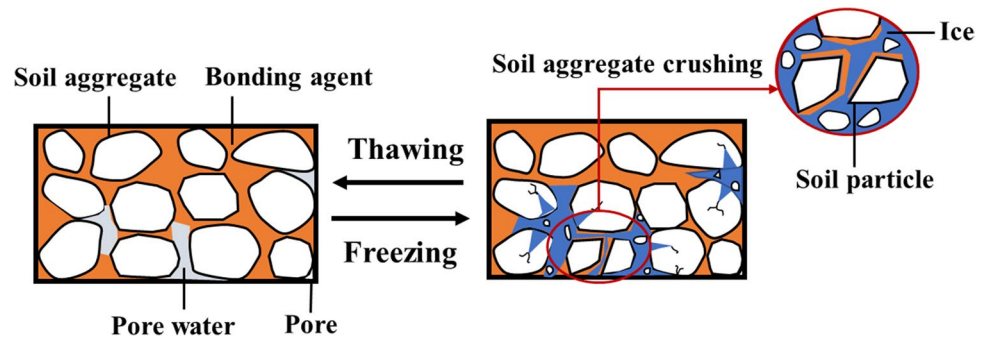**Fig. 5** Schematic diagram of soil structure failure during freezing and thawing

Table 6 Hydration of cement

Mineral	Chemical composition	Content (wt%)	Hydration reaction process
Tricalcium silicate (C$_3$S)	$3CaO \cdot SiO_2$	36~60	$2(3CaO \cdot SiO_2) + 6H_2O$ $\rightarrow 3CaO \cdot 2SiO_2 \cdot 3H_2O + 3Ca(OH)_2$
Dicalcium silicate (C$_2$S)	$3CaO \cdot SiO_2$	15~36	$2(2CaO \cdot SiO_2) + 6H_2O$ $\rightarrow 3CaO \cdot 2SiO_2 \cdot 3H_2O + 3Ca(OH)_2$
Tricalcium aluminate (C$_3$A)	$3CaO \cdot Al_2O_3$	7~15	$3CaO \cdot Al_2O_3 + 6H_2O \rightarrow 3CaO \cdot Al_2O_3 \cdot 6H_2O$
Tetra-calcium aluminoferrite (C$_4$AF)	$4CaO \cdot Al_2O_3 \cdot Fe_2O_3$	10~18	$4CaO \cdot Al_2O_3 \cdot Fe_2O_3 + 2Ca(OH)_2 + 10H_2O$ $\rightarrow 3CaO \cdot Al_2O_3 \cdot 6H_2O + 3CaO \cdot Fe_2O_3 \cdot 6H_2O$

Table 7 Main chemical reactions of lime in the remediation system

Reaction	Product	Reaction equation	Note
Lime slaking	$Ca(OH)_2$	$CaO + H_2O \rightarrow Ca(OH)_2$	Exothermic reaction, promoting other reactions in system
Ion exchange	$Pb(OH)_2$	$Ca(OH)_2 \rightarrow Ca^{2+} + 2OH^-$ $Pb^{2+} + 2OH^- \rightarrow Pb(OH)_2$	Solidification of Pb^{2+}
Carbonization	$CaCO_3$	$Ca(OH)_2 + CO_2 \rightarrow CaCO_3 + H_2O$	Limestone, improving soil strength
Pozzolanic reactions	$Ca_5Si_6O_{16}(OH) \cdot 4H_2O$		Calcium silicate hydrate, calcium aluminate hydrate, and other gels improving soil strength

Table 8 Pozzolanic reaction of fly ash

Reaction	Product	Reaction equation	Note
Pozzolanic reactions	CSH, CAH	$Ca(OH)_2 \rightarrow Ca^{2+} + 2OH^-$ $Ca^{2+} + 2OH^- + SiO_2 \rightarrow CSH$ $Ca^{2+} + 2OH^- + Al_2O_3 \rightarrow CAH$	Active SiO_2 and Al_2O_3 combine with CaO in the cement and lime to produce hydraulic binders

in fly ash leads to its weak hydration; however, the total content of silica and alumina in fly ash exceeds 50%, and once mixed with the cement and/or lime, active silica and alumina in fly ash will react with calcium oxide provided by cement and lime to form a gel (Nie 2013). Moreover, the microbead structure of the fly ash accelerates the hydration and carbonation reactions by increasing the active surface energy of the specimen (Wu 2013). Activated carbon in fly ash facilitates heavy metal adsorption, thereby weakening the hindrance of heavy metal ions to the hydration of curing

agents (Gao 2004). All these elements might help to improve the strength and stability of fly ash-containing Pb-CSCS under long-term F-T.

Nevertheless, a lower strength of C2.5S5F5 compared to that of C5S5 at 0.5% lead content and subjected to 3 and 7 F-T was found (Fig. 6a). It reveals that the cement in the curing agent still played a dominant role in the UCS of the specimen under low lead content and short-term F-T conditions. Conversely, lime has 1.45 times more calcium oxide than cement, ionizing a large amount of hydroxide ions in
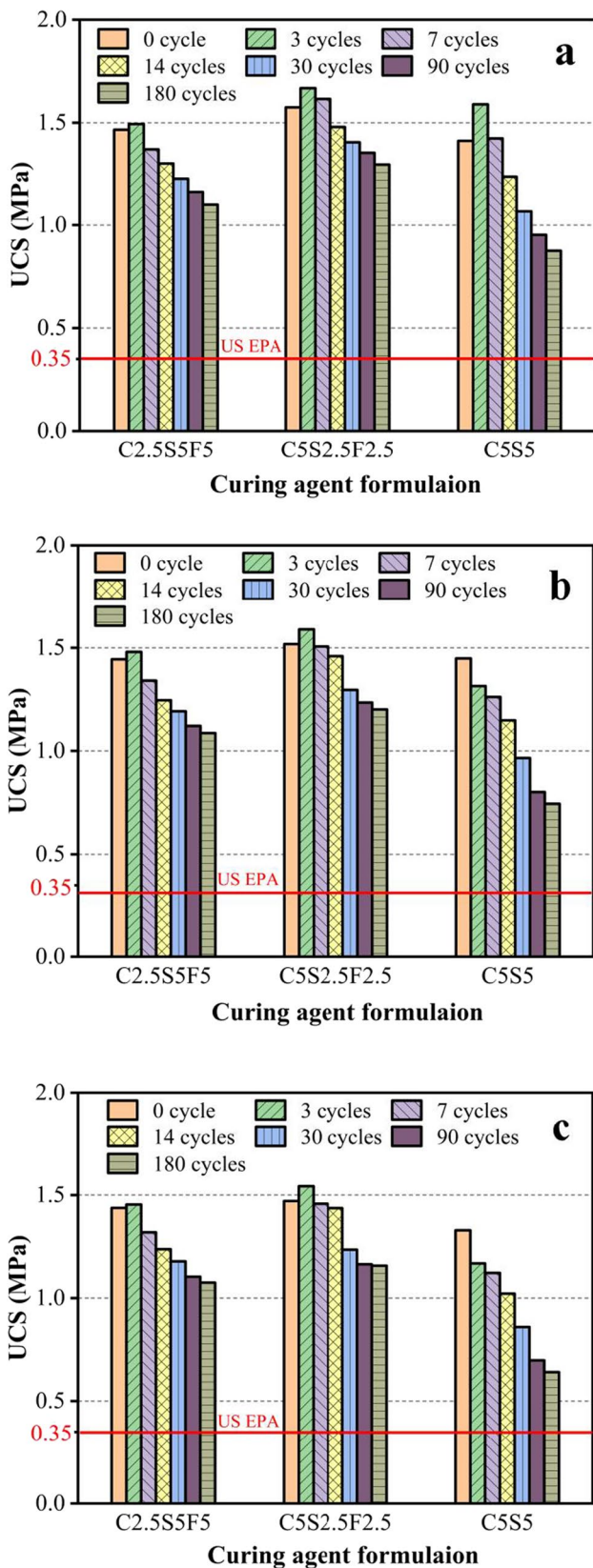
Fig. 6 UCS of Pb-CSCS with varying curing agent formulations under F-T: **a** Pb 0.5%, **b** Pb 1%, and **c** Pb 1.5%

an aqueous environment. This means that in the case of high lead content, more lead precipitates were generated and coated on the surface of curing agent particles to hinder hydration, and macroscopically, the UCS of Pb-CSCS with high lime content were lower.

The effect of lead concentration

Figure 7 illustrates the effects of lead content on the UCS of the specimens at different F-T times. UCS decreased with increasing lead content, which is due to the fact that lead ions have a greater binding ability with hydration products compared with calcium ions generated by the hydrolysis of curing agent to stabilize itself (Yousuf et al. 1995). While excessive lead ions bind directly to the mineral crystal lattice of hydration products, resulting in structural disruption in hydration products (G and J 1999; Horpibulsuk et al. 2012). Significantly, Pb-CSCS with a higher cement content was more susceptible to deterioration. This is owing to the fact that the level of lead content in solidified lead-contaminated soil samples not only hinders the initial and final setting time of the cement hydration reaction but also directly reduces the strength of gels, thereby causing a strength reduction of the solidified soil (Olmo et al. 2001).

Upon short-term F-T of 3 cycles (Fig. 7b) or 7 cycles (Fig. 7c), the UCS of C5S5 was higher than that of C2.5S5F5 at a low lead level (0.5%), while the opposite was found at higher lead levels. The inversion indicates that changes in lead content could affect the strength stability of Pb-CSCS with a given curing agent formulation in the freezing–thawing environment. However, that did not occur for Pb-CSCS subjected to a longer F-T time (Fig. 7d–g). There might be quite different main factors that affect the UCS of specimens with different F-T durations. Specifically, the main influencing factor is shifted from the hydration of curing agents under short-term F-T to the structural damage of the specimen by F-T under long-term F-T.

ANOVA ANOVA tests were performed to clarify the main influencing factors that control the UCS evolution of Pb-CSCS suffering from different F-T durations. The results showed that factors A, B, and C all had a certain degree of influence on the UCS of the Pb-CSCS in both short- and long-term F-T cases, as the values of p were all < 0.01. The relationship strengths (R^2) of the investigated factors on the UCS for the short-term F-T (Fig. 8a) were 26% (factor A), 44% (factor B), and 14% (factor C), respectively. Curing agent formulation (factor B) has had the most significant effect on UCS. It was further found that C5S2.5F2.5 had the largest effect size ($\hat{\alpha}_i = 127.5$), whereas that of C5S5 ($\hat{\alpha}_i = -110.3$) was the smallest. This is consistent with the test results, where the UCS of C5S2.5F2.5 was generally the highest and that of C5S5 was the lowest under the same con-

**Fig. 7** UCS of Pb-CSCS with varying lead concentration under F-T
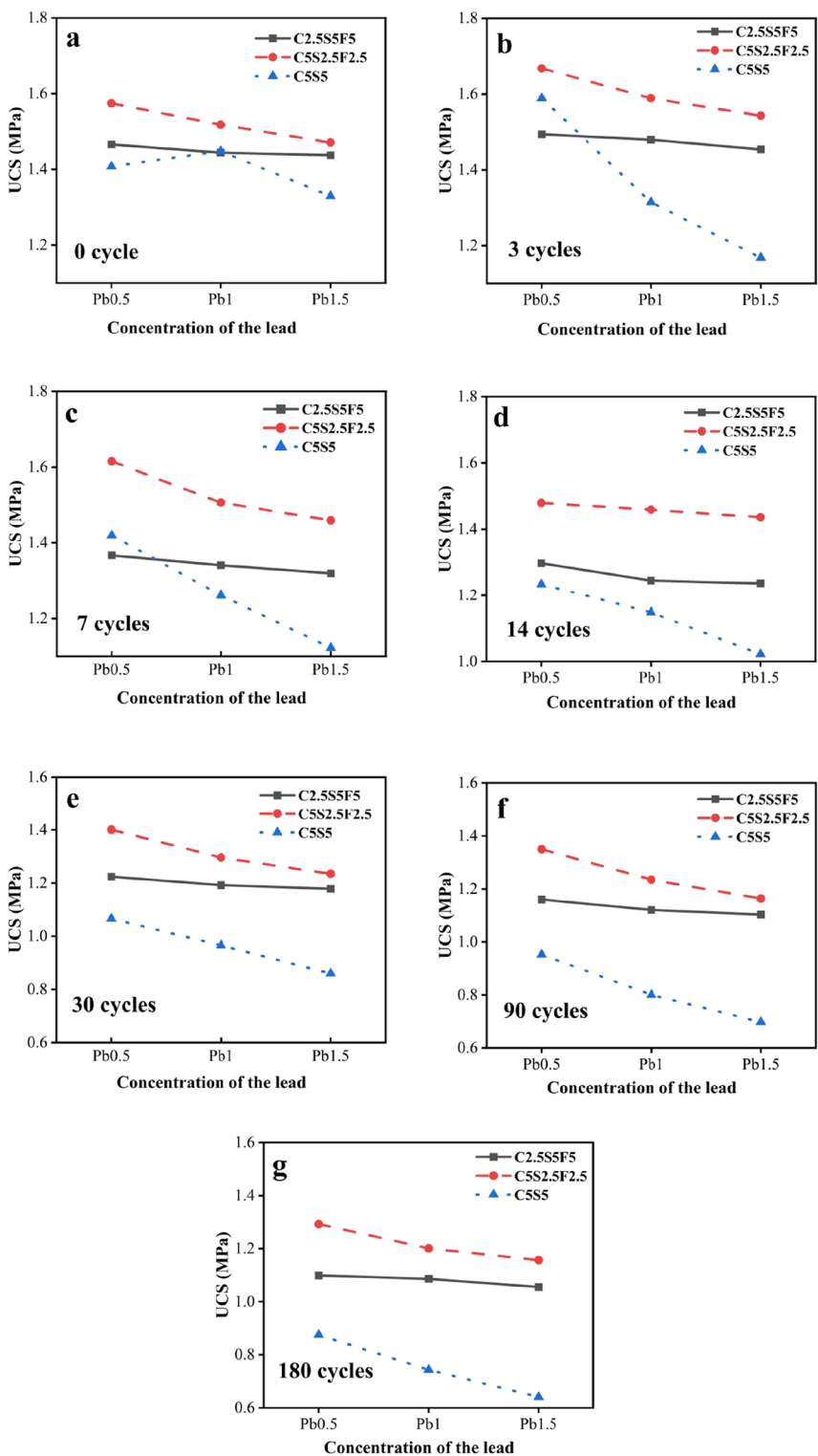
ditions, due to the positive effects of the presence of fly ash and the highest cement and lower lime content as analyzed in the "The effect of curing agent formulation" section.

Different conclusions could be drawn for the long-term F-T, where F-T duration (factor A) became the most influential one on UCS with a relationship strength of 51%

(Fig. 8b). The effect size of level 1 (0 F-T) was the largest among the four levels at 281. This also agrees with the test results where UCS was the highest when suffering no F-T compared to the other long-term F-T levels (30, 90, and 180 F-T). Again, the fact that the main influencing factors of the UCS of Pb-CSCS shifted from the hydration

Fig. 8 Relationship strength (R^2) of the factors on the UCS of Pb-CSCS under F-T: **a** 0 ~ 14 F-T and **b** 0 ~ 180 F-T
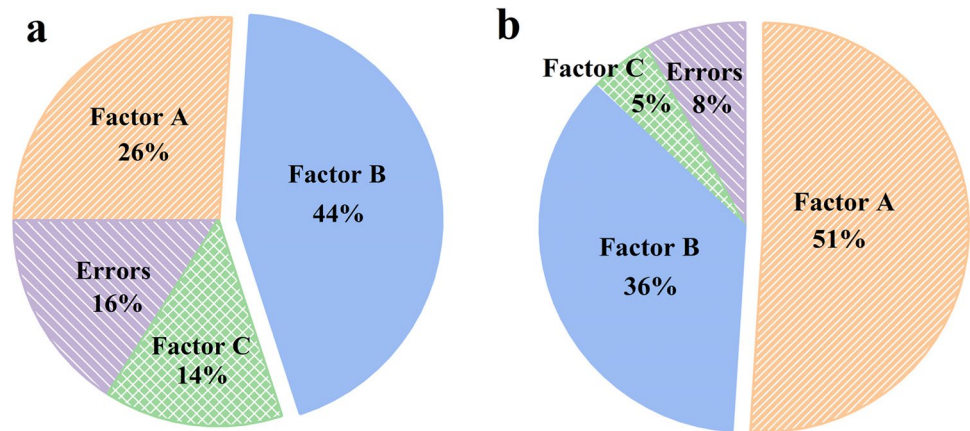
of curing agents under short-term F-T to the impact of F-T on the soil structure under long-term F-T.

Lead leaching characteristics of Pb-CSCS under long-term F-T

Leachate pH

Leachate pH provides information on the chemical stability of Pb-CSCS (1% lead) during semi-dynamic leaching (Fig. 9). The overall variations of the leachate pH of Pb-CSCS with different curing formulations were similar. In the initial stage of leaching, the overall increase in the pH values of the leachate was mainly due to the neutralization of the acid leaching solution with the alkalis generated by the hydrolysis of the curing agent in Pb-CSCS. Alkalis on the near soil surface were gradually consumed as the neutralization reaction continued. Continued renewal of the acid leaching solution caused a subsequent decrease in the leachate pH. After the hydration products on the surface of the specimens were destroyed by acid erosion, the leaching solution started getting inside the soil body through the pores and cracks. This allowed the internal alkalis to dissolve into the leaching solution and showed a slow increase in pH again. As the available alkalis were depleted, the leachate pH eventually dropped sharply due to the deteriorated acid resistance of Pb-CSCS from the acid leaching.

Notably, the leachate pH of C5S5 (0% fly ash) was clearly higher than that of C2.5S5F5 (40% fly ash) and C5S2.5F2.5 (25% fly ash), and changes gently with the increasing F-T. This demonstrates that the specimens with a higher proportion of cement and lime in the curing agent have better frost resistance and acid resistance. Instead, fly ash significantly reduces the frost resistance and acid resistance of the specimens. This is in line with the conclusion that fly ash reduces the acid–base buffering capacity of solidified waste (Li et al. 2001).

It was also found that the leachate pH of Pb-CSCS subjected to a shorter F-T duration was overall higher. A shorter F-T duration means a shorter time for hydration of agents and thus more unreacted gel-forming alkalis that are susceptible to neutralization reactions. Correspondingly, longer F-T durations allowed for more adequate hydration of the agents, forming more gels for greater soil acid resistance. Therefore, pH fluctuations were reduced for Pb-CSCS after a longer F-T duration, and the pH change nodes were delayed compared to those after a shorter F-T duration.
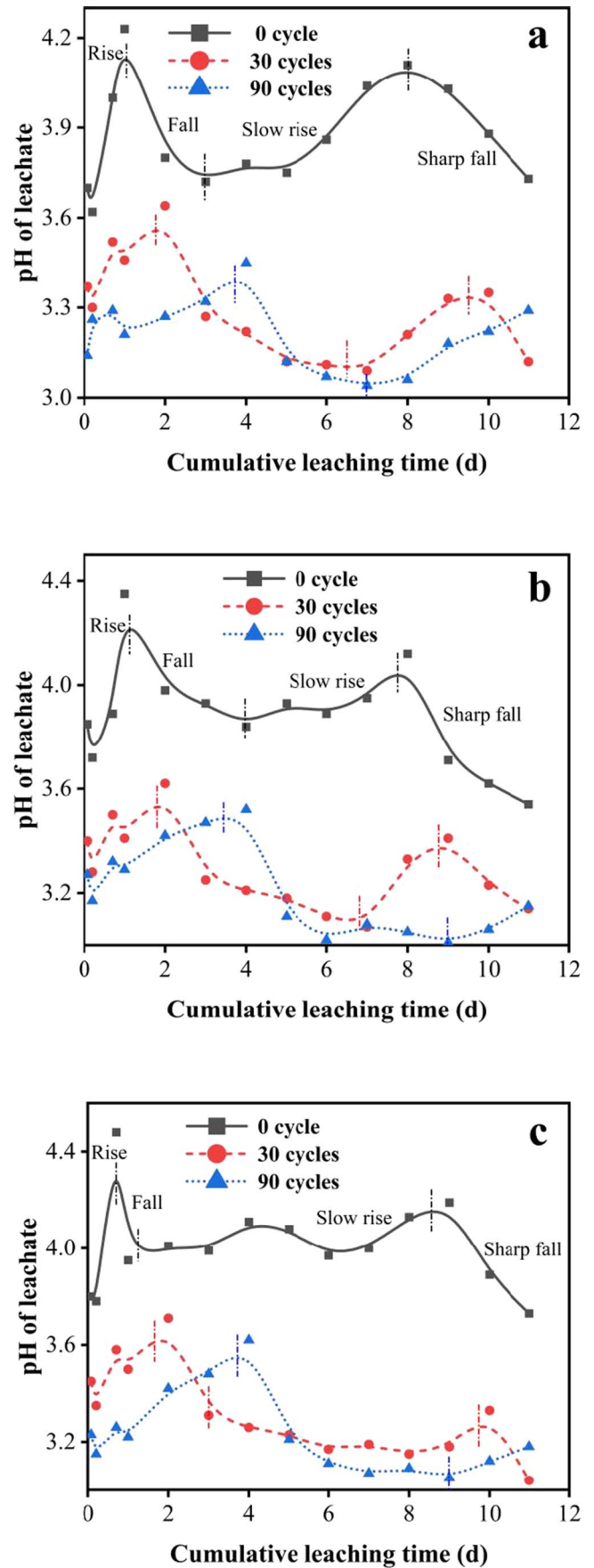
Leaching concentration of lead

Lead concentrations in leachate for all the three types of Pb-CSCS after F-T showed an overall pattern of an initial increase followed by a decrease, and finally remaining relatively stable with leaching time (Fig. 10). For Pb-CSCS with a specific curing agent formulation, the peak value of lead concentration was higher after a longer F-T, and a larger cumulative leaching time was required to reach the peak. The structural damage of Pb-CSCS by F-T allows the leaching solution to penetrate deeper into the soil mass, making more internal immobilized lead available for leaching. Correspondingly, it takes more time to fully enter the internal soil and leach the available lead out. More intuitively, Fig. 11 shows the phenomenon that the cumulative leaching mass of lead increased almost linearly with the increase in freeze–thaw time. The increase in cement and lime corporations reduced the cumulative lead leaching mass. A large amount of calcium oxide in the system provided by cement and especially lime enhanced the soil acid resistance (Li et al. 2001), which is beneficial to heavy metal stabilization.

The effective diffusion coefficient of lead

The effective diffusion coefficient (D_e) is often used to evaluate the mobility of substances in porous media. D_e of lead in Pb-CSCS under F-T ranged from 3.86×10^{-13} to

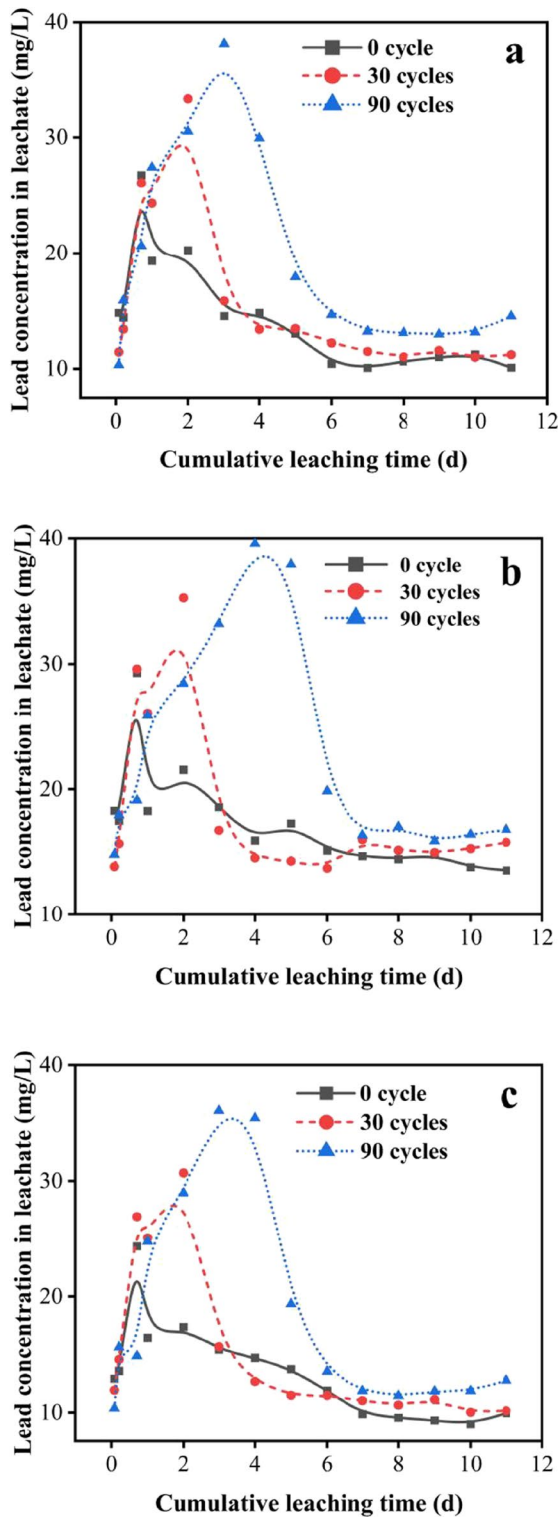**Fig. 9** Leachate pH of Pb-CSCS with acid leaching under F-T: **a** C2.5S5F5, **b** C5S2.5F2.5, and **c** C5S5

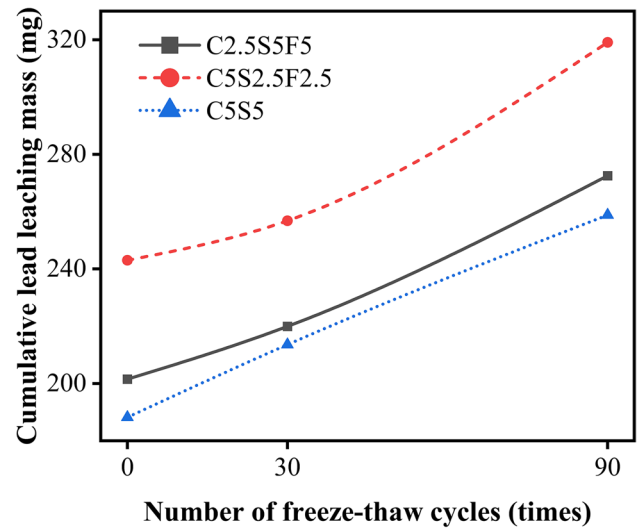Fig. 10 The concentration of lead in the leachate of Pb-CSCS under F-T: **a** C2.5S5F5, **b** C5S2.5F2.5, and **c** C5S5

Fig. 11 Cumulative lead leaching mass of Pb-CSCS under F-T
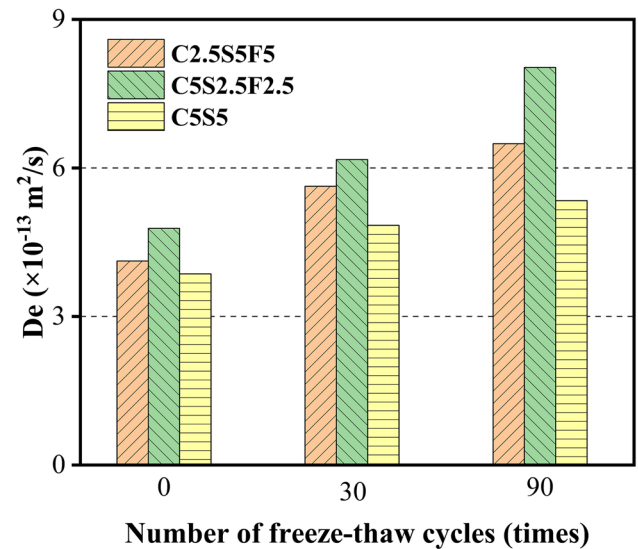
Fig. 12 The effective diffusion coefficient of lead in Pb-CSCS under F-T

8.03×10^{-13} m^2/s (Fig. 12), which is within the common order of magnitude for that of lead in solidified/stabilized lead-contaminated soils ($10^{-19} \sim 10^{-12}$ m^2/s). According to the existing classification of the mobility of heavy metals in polluted soil abased on D_e ($D_e < 3.0 \times 10^{-13}$ m^2/s, low mobility; $3.0 \times 10^{-13} \leq D_e < 1.0 \times 10^{-12}$ m^2/s, medium mobility; and $D_e \geq 1.0 \times 10^{-12}$ m^2/s, high mobility), all the tested Pb-CSCS indicated medium mobility of lead under acid leaching. Lead mobility in Pb-CSCS with C5S2.5F2.5 was the largest, followed by C2.5S5F5, and that of C5S5 was the smallest under the same conditions, which corresponded to their cumulative lead leaching mass. Once again, it confirms that the samples with higher cement and lime content have a better curing effect of lead, and the lime offers the greater benefit. In addition, D_e increased with longer F-T durations.

The enhanced lead migration demonstrated the deteriorating effect of freezing–thawing on the structural integrity of solidified soil from another perspective next to soil strength.

SEM

Figure 13 displays SEM images of the Pb-CSCS with varying curing agent formulation at 0.5% lead under F-T. The surface of the hydrated gel became rougher and more porous in the soil as the F-T times increased. This indicates that the F-T has a significant damaging effect on the soil structure. When the F-T time was increased to 180 d, a large number of acicular bacillus cement (commonly referred to as ettringite (AFt)) was observed. The swelling of AFt in water led to a loss of strength, which accelerated the physical deterioration of Pb-CSCS. Furthermore, flaky calcium hydroxide and gel-like CSH/CAH production was observed in the samples that subjected to 3 F-T. This is consistent with the conclusion that short-term F-T promotes the hydrolysis of the curing agent and thus increases the early strength of the Pb-CSCS.

Figure 14a–d depict the entire process of the gradual reaction of the fly ash surface to produce the gelling substance CAH/CSH. This phenomenon also corresponds to the fact that fly ash improves the strength development and stability of Pb-CSCS under long-term F-T. Compared to Fig. 14b, less cementitious material is produced in Fig. 14d, which also shows that the high content of lead slows down the hydration reaction of the cement.

Conclusions

This study focused on the strength and chemical stability of Pb-CSCS under long-term F-T conditions via UCS and semi-dynamic leaching tests. The effects of three influential factors, F-T duration, curing agent formulation, and lead content, on the research properties were investigated. The influence strength of each factor on the UCS of Pb-CSCS under different F-T durations was clarified mathematically by ANOVA. The main conclusions include:

(1). Short-term F-T facilitated the strength improvement of Pb-CSCS, but the deterioration of Pb strength was eventually highlighted after long-term freeze–thaw. The most influential factor on the UCS of Pb-CSCS shafted from the curing agent hydration during the short-term F-T to the structural damage by the later-stage F-T.

(2). Cement dominated the UCS of Pb-CSCS with low lead content under short-term F-T, while fly ash improved the strength development and stability of Pb-CSCS under long-term F-T.

(3). Lead degraded soil strength by generating precipitation that hindered hydration of the curing agent and directly degraded the gel strength, especially for the Pb-CSCS with high lime content.

(4). The mobility of lead in Pb-CSCS was medium under acid leaching, and it increased as freeze–thaw pro-

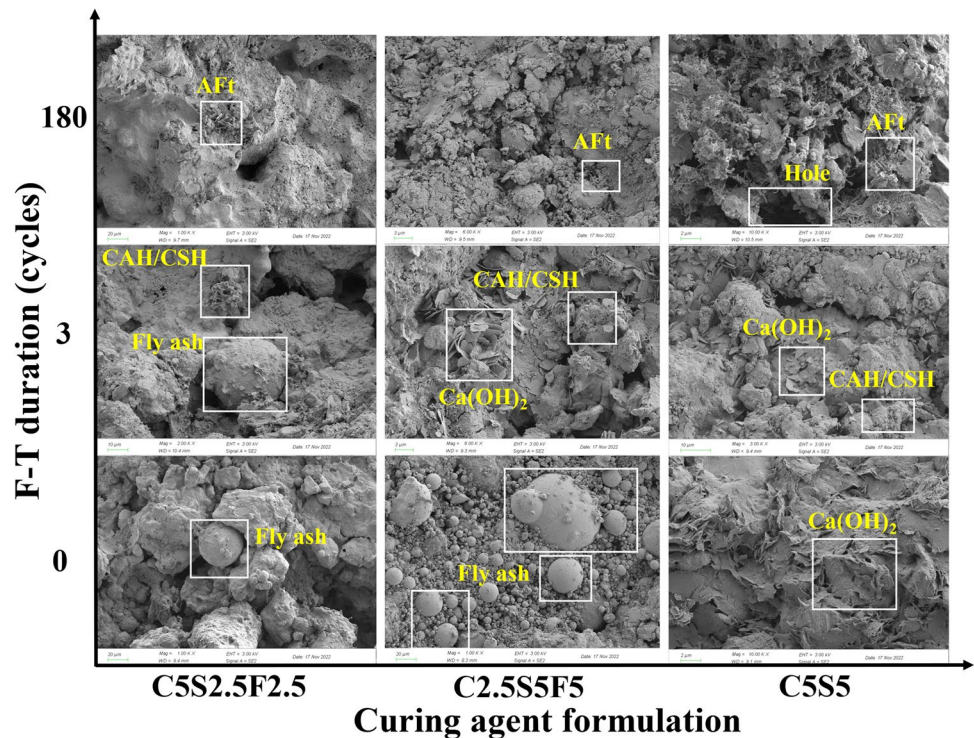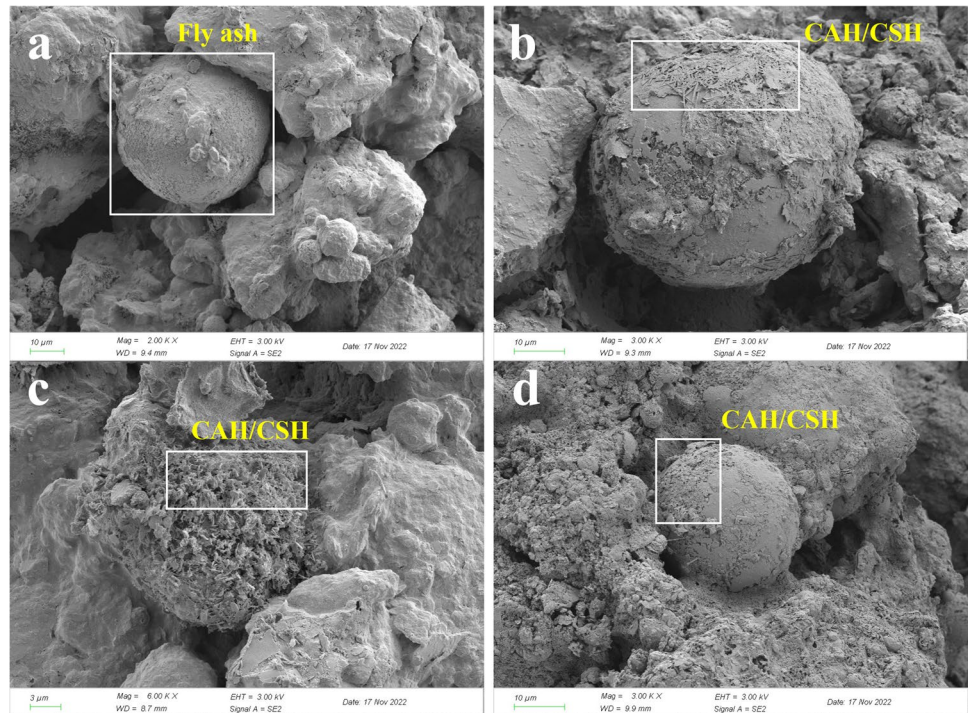**Fig. 13** SEM images of Pb-CSCS with varying curing agent formulations at 0.5% lead under F-T

Fig. 14 SEM images of Pb-CSCS with C5S2.5F2.5: with 0.5% lead and **a** 0 F-T, **b** 3 F-T, and **c** 180 F-T; with 1.5% lead and **d** 3 F-T

gressed. Higher cement content, especially lime content in curing agents, favored the stabilization of lead.

Overall, the findings showed the long-term performance and failure mechanism of Pb-CSCS with a view to providing guidance for engineering construction on the remediated site and the control of secondary contamination risks, as well as a reference for the selection of suitable curing agents and proportioning. Undeniably, due to the vast, complex conditions in the field, additional heavy metal species and the safety of curing agents should be considered. In situ tests should be conducted if necessary to evaluate the remediation effect from multiple perspectives and indicators.

Declarations

Ethics approval Not applicable.

Consent to participate Not applicable.

Consent to publish Not applicable.

Competing interests The authors declare no competing interests.

References

Aldaood A, Bouasker M, Al-Mukhtar M (2014) Impact of freeze–thaw cycles on mechanical behaviour of lime stabilized gypseous soils. Cold Reg Sci Technol 99:38–45

American National Standards Institute (2019) Measurement of the leachability of solidified low level radioactive wastes by a short-term test procedure, USA

American Society for Testing and Materials (2008) Standard test method for accelerated leach test for diffusive releases from solidified waste and a computer program to model diffusive, fractional leaching from cylindrical waste forms, Philadelphia, USA

Ashraf S, Ali Q, Zahir ZA, Ashraf S, Asghar HN (2019) Phytoremediation: Environmentally sustainable way for reclamation of heavy metal polluted soils. Ecotoxicol Environ Saf 174:714–727

Bai B, Jiang S-C, Liu L-L, Li X, Wu H-Y (2021a) The transport of silica powders and lead ions under unsteady flow and variable injection concentrations. Powder Technol 387:22–30

Bai B, Nie Q-K, Zhang Y-K, Wang X-L, Hu W (2021b) Cotransport of heavy metals and SiO_2 particles at different temperatures by seepage. J Hydrol 597:125771

Brady NC, Weil RR (2016) The nature and properties of soils. Person, USA

China Association of Environmental Protection Industry (2020) Soil and groundwater remediation industry development report 2019 (in Chinese)

Cao X, Zhang Q, Yang W, Fang L, Liu S, Ma R, Guo K, Ma N (2023) Lead-chlorine synergistic immobilization mechanism in municipal

solid waste incineration fly ash (MSWIFA)-based magnesium potassium phosphate cement. J Hazard Mater 442: 130038

Cao Z-G, Zhang D-W, Liu S-Y (2013) Experimental research on durability of solidified lead-contaminated soils under wetting-drying cycles. Rock Soil Mech 34:3485–3490

Chen SS, Taylor JS, Baek K, Khan E, Tsang DCW, Ok YS (2017) Sustainability likelihood of remediation options for metal-contaminated soil/sediment. Chemosphere 174:421–427

Deng R-F (2017) Effects of freezing and thawing cycles on engineering properties of cement stabilized lead contaminated soil and its mechanism, Chongqing University (in Chinese)

Dermatas D, Meng X-G (2003) Utilization of fly ash for stabilization/solidification of heavy metal contaminated soils. Eng Geol 70:377–394

Ding M-T, Zhang F, Ling X-Z, Lin B (2018) Effects of freeze-thaw cycles on mechanical properties of polypropylene Fiber and cement stabilized clay. Cold Reg Sci Technol 154:155–165

Du Y-J, Jiang N-J, Shen S-L, Jin F (2012) Experimental investigation of influence of acid rain on leaching and hydraulic characteristics of cement-based solidified/stabilized lead contaminated clay. J Hazard Mater 225:195–201

Du Y-J, Wei M-L, Reddy KR, Liu Z-P, Jin F (2014) Effect of acid rain pH on leaching behavior of cement stabilized lead-contaminated soil. J Hazard Mater 271:131–140

Eskişar T, Altun S, Kalıpcılar İ (2015) Assessment of strength development and freeze–thaw performance of cement treated clays at different water contents. Cold Reg Sci Technol 111:50–59

G. T, J. P (1999) Interactions between lead and different binders. Cem Concr Res 29:1605-1610

Gao H-R (2021) Methodology study of frozen soil monitoring and simulation based on remote sensing and numerical model. Dissertation, University of Chinese Academy of Sciences (in Chinese)

Gao J-W, Yu H-M, Li K (2014) Experimental research on unconfined compression strength of loess. Saf Environ Eng 21:132–137 (in Chinese)

Gao Y-L (2004) Solid waste treatment and disposal with engineering examples. China building materials industry press, Beijing (in Chinese)

Gong Y-Y, Zhao D-Y, Wang Q-L (2018) An overview of field-scale studies on remediation of soil contaminated with heavy metals and metalloids: Technical progress over the last decade. Water Res 147:440–460

Gu F, Zhang J, Shen Z, Li Y, Ji R, Li W, Zhang L, Han J, Xue J, Cheng H (2022) A review for recent advances on soil washing remediation technologies. Bull Environ Contam Toxicol 109:651–658

Guo P (2015) Principle and application of three factors analysis of variance. J Shenyang Univ (natural Science) 27:40–43 (in Chinese)

He L, Wang Z, Gu W-B (2021) Evolution of freeze–thaw properties of cement–lime solidified contaminated soil. Environ Technol Innov 21: 101189

Horpibulsuk S, Phojan W, Suddeepong A, Chinkulkijniwat A, Liu MD (2012) Strength development in blended cement admixed saline clay. Appl Clay Sci 55:44–52

Hotineanu A, Bouasker M, Aldaood A, Al-Mukhtar M (2015) Effect of freeze–thaw cycling on the mechanical properties of lime-stabilized expansive clays. Cold Reg Sci Technol 119:151–157

Hou D-Y, Al-Tabbaa A (2014) Sustainability: a new imperative in contaminated land remediation. Environ Sci Policy 39:25–34

Hou D-Y, Gu Q-B, Ma F-J, O'Connell S (2016) Life cycle assessment comparison of thermal desorption and stabilization/solidification of mercury contaminated soil on agricultural land. J Clean Prod 139:949–956

Hou D-Y, O'Connor D, Igalavithana AD, Alessi DS, Luo J, Tsang DCW, Sparks DL, Yamauchi Y, Rinklebe J, Ok YS (2020a) Metal contamination and bioremediation of agricultural soils for food safety and sustainability. Nat Rev Earth Environ 1:366–381

Hou R-J, Wang L-W, O'Connor D, Tsang DCW, Rinklebe J, Hou D-Y (2020b) Effect of immobilizing reagents on soil Cd and Pb lability under freeze-thaw cycles: Implications for sustainable agricultural management in seasonally frozen land. Environ Int 144:106040

Institute for Health Metrics and Evaluation (2020) The toxic truth: children's exposure to lead pollution undermines a generation of future potential, Unicef

Kumar A, Kumar A, M MSC, Chaturvedi AK, Shabnam AA, Subrahmanyam G, Mondal R, Gupta DK, Malyan SK, S SK, S AK,Yadav KK (2020): Lead toxicity: health hazards, influence on food chain, and sustainable remediation approaches. Int J Environ Res Public Health 17:2179

Li D-H (2019a) Study on degradation of engineering characteristics and mechanisms of compound solidified lead contaminated soil characteristics under freeze-thaw cycles. Dissertation, Chongqing University (in Chinese)

Li S (2019b) Soil and groundwater remediation industry development report (2018) (in Chinese)

Li X-D, C.S. P, Sun H, I.M.C. L, D.W. K (2001) Heavy metal speciation and leaching behaviors in cement based solidified/stabilized waste materials. J Hazard Mater 82:215-230

Li J-S, Xue Q, Wang P, Li Z-Z, Liu L (2014) Effect of drying-wetting cycles on leaching behavior of cement solidified lead-contaminated soil. Chemosphere 117:10–13

Li X-J, Yang R-Z, Li H, Yi H, Jing H-J (2021) Experimental study on solidification and stabilization of heavy-metal-contaminated soil using cementitious materials. Materials (Basel) 14:4999

Liu J-J (2014) The stability of solidified/stabilized heavy metal contaminated soils under erosive environment. Dissertation, Hefei University of Technology (in Chinese)

Liu J-J, Zha F-S, Hao A-L, Zhang X-Q, Cui K-R (2015): Strength and leaching characteristics of chromium polluted soil solidified with cement in a NaCl erosion environment. Rock Soil Mech 36:2855–2861+2876 (in Chinese)

Liu J-J, Zha F-S, Xu L, Kang B, Tan X-H, Deng Y-F, Yang C-B (2019) Mechanism of stabilized/solidified heavy metal contaminated soils with cement-fly ash based on electrical resistivity measurements. Measurement 141:85–94

Liu J, Zhao L, Liu Q, Li J, Qiao Z, Sun P, Yang Y (2022) A critical review on soil washing during soil remediation for heavy metals and organic pollutants. Int J Environ Sci Technol 19:601–624

Liu P, Zhang Y, Tang Q, Shi S (2021a) Bioremediation of metal-contaminated soils by microbially-induced carbonate precipitation and its effects on ecotoxicity and long-term stability. Biochem Eng J 166:107856

Liu S-J, Miao C, Yao S-S, Ding H, Zhang K (2021b) Soil stabilization/solidification (S/S) agent—water-soluble thiourea formaldehyde (WTF) resin: Mechanism and performance with cadmium (II). Environ Pollut 272:116025

Liu Z-P, Du Y-J, Jiang N-J, Zhu J-J (2013) Leaching properties of cement-solidified lead-contaminated clay via semi-dynamic leaching tests. Chin J Geotech Eng 35:2212–2218 (in Chinese)

Nie Y-F (2013) Solid waste disposal engineering manual. Chemical Industry Press, Beijing (in Chinese)

Olmo IFn, Chacon E, Irabien A (2001) Influence of lead, zinc, iron (III) and chromium (III) oxides on the setting time and strength development of Portland cement. Cem Concr Res 31:1213-1219

Ouhadi VR, Yong RN, Deiranlou M (2021) Enhancement of cement-based solidification/stabilization of a lead-contaminated smectite clay. J Hazard Mater 403:123969

Peng X-Q (2006) Civil engineering materials. Chongqing University Press, Chongqing (in Chinese)

Pervaiz A, Zhong Q, Rehman SAU, Ma C, Jiao Y, He M (2023) Immobilization and phytoavailability of antimony (Sb) in contaminated agricultural soils amended with composted manure. Sci Total Environ 856: 159213

Pu H-F, Mastoi AK, Chen X-L, Song D-B, Qiu J-W, Yang P (2020) An integrated method for the rapid dewatering and solidification/stabilization of dredged contaminated sediment with a high water content. Front Environ Sci Eng 15:67 (in Chinese)

Shahidi M, Farrokhi F, Asemi F (2019) Changes in physical and mechanical properties of gas oil–contaminated clayey sand after addition of clay nanoparticles. J Environ Eng 145:04019004

Sharma M, Satyam N, Reddy KR (2020) Strength enhancement and lead immobilization of sand using consortia of bacteria and blue-green algae. J Hazard Toxic Radioact Waste 24:04020049

Shen Y, Zhang W-H (2013) Geotechnical testing technology. Metallurgical industry press, Beijing (in Chinese)

Shen Z-T, Jin F, O'Connor D, Hou D-Y (2019) Solidification/stabilization for soil remediation: an old technology with new vitality. Environ Sci Technol 53:11615–11617

Tang J-Y, Zhang J-C, Ren L-H, Zhou Y-Y, Gao J, Luo L, Yang Y, Peng Q-H, Huang H-L, Chen A-W (2019) Diagnosis of soil contamination using microbiological indices: A review on heavy metal pollution. J Environ Manage 242:121–130

USEPA (1996) Prohibition on the disposal of bulk liquid hazardous waste in landfills – Statutory Interpretive Guidance, Washington

Wang F, Zhang Y-H, Shen Z-T, Pan H, Xu J, Al-Tabbaa A (2019) GMCs stabilized/solidified Pb/Zn contaminated soil under different curing temperature: leachability and durability. Environ Sci Pollut Res Int 26:26963–26971

Wang J, Zeng G, Deng H, Liu X, Zhao D (2022) Microwave-enhanced simultaneous immobilization of lead and arsenic in a field soil using ferrous sulfate. Chemosphere 305:136388

Wang L, Yu K-Q, Li J-S, Tsang DCW, Poon CS, Yoo J-C, Baek K, Ding S-M, Hou D-Y, Dai J-G (2018) Low-carbon and low-alkalinity stabilization/solidification of high-Pb contaminated soil. Chem Eng J 351:418–427

Wang T-L, LIiu J-K, Tian Y-H (2011): Static properties of cement- and lime-modified soil subjected to freeze-thaw cycles. Rock Soil Mech 32:193-198 (in Chinese)

Wang T-l, Liu Y-j, Yan H, Xu L (2015) An experimental study on the mechanical properties of silty soils under repeated freeze–thaw cycles. Cold Reg Sci Technol 112:51–65

Wang X, Zhong D-L, Hou H-J, Gu Q-B, Yang R, Chen J, Yang J-K, Wang L-L (2016) Catalytic degradation of PNP and stabilization/solidification of Cd simultaneously in soil using microwave-assisted Fe-bearing attapulgite. Chem Eng J 304:747–756

Wei H-B, Jiao Y-B, Liu H-B (2015a) Effect of freeze–thaw cycles on mechanical property of silty clay modified by fly ash and crumb rubber. Cold Reg Sci Technol 116:70–77

Wei M-L, Du Y-J, Reddy KR, Wu H-L (2015b) Effects of freeze-thaw on characteristics of new KMP binder stabilized Zn- and Pb-contaminated soils. Environ Sci Pollut Res Int 22:19473–19484

Wiles C (1987) A review of solidification stabilization technology. J Hazard Mater 14:5–21

Wu Z-Z (2013) Comprehensive utilization of fly ash. China building materials industry press, Beijing (in Chinese)

Yang N-R (2003) C-S-H gel and its determination methods. Bull Chin Ceram Soc 2:46–52 (in Chinese)

Yang Z-P, Li D-H, Deng R-F, Tian X, Ren S-P (2019) An experimental study for influence of freeze-thaw cycles on strength and pore characteristics of solidified lead-contaminated soil. J Eng Geol 27:539–549 (in Chinese)

Yang Z-P, Li X-Y, Li D-H, Wang Y, Liu X-R (2020a) Effects of long-term repeated freeze-thaw cycles on the engineering properties of compound solidified/stabilized Pb-contaminated soil: deterioration characteristics and mechanisms. Int J Environ Res Public Health 17:1798

Yang Z-P, Wang Y, Li D-H, Li X-Y, Liu X-R (2020b) Influence of freeze–thaw cycles and binder dosage on the engineering properties of compound solidified/stabilized lead-contaminated soils. Int J Environ Res Public Health 17:1077

Yang Z, Chang J, Wang Y, Li X, Li S (2021) Effects of long-term freeze–thaw cycles on the properties of stabilized/solidified lead-zinc-cadmium composite-contaminated soil. Int J Environ Res Public Health 18:6114

Yi Y-L, Liska M, Al-Tabbaa A (2012) Initial Investigation into the use of GGBS-MgO in Soil Stabilisation. Proceedings of the fourth international conference on grouting and deep mixing: 444–453, New Orleans

Yousuf M, Mollah A, Vempati RK, Lin T-C, Cocke DL (1995) The interfacial chemistry of solidification-stabilization of metals in cement and pozzolanic material systems. Waste Manage 15:137–148

Yu A-M, Xu T-Q (2018) Research on formation mechanism of limestone soil strength. North Commun 10:61–63 (in Chinese)

Yu Z-R, Yu Y-C, Gao Y-Y, Zhou Z-Y (1989) The application and mechanism of lime in sludge conditioning. China Water Wastewater 5:7-11 (in Chinese)

Zha F-S, Liu J-J, Xu L, Cui K-R (2013) Effect of cyclic drying and wetting on engineering properties of heavy metal contaminated soils solidified/stabilized with fly ash. J Cent South Univ 20:1947–1952

Zhang Y-H, Hou D-Y, O'Connor D, Shen Z-T, Shi P-L, Ok YS, Tsang DCW, Wen Y, Luo M-N (2019) Lead contamination in Chinese surface soils: source identification, spatial-temporal distribution and associated health risks. Crit Rev Environ Sci Technol 49:1386–1423

Zheng X, Li Q, Peng H, Zhang J, Chen W, Zhou B (2022) Remediation of heavy metal-contaminated soils with soil washing: a review. Sustainability 14(20):13058

Zhong B, Liu Q-S, Liu C-L (2015) Mathematical statistics. Higher education press, Beijing (in Chinese)